Biomaterials 210 (2019) 51–61

Contents lists available at ScienceDirect

Biomaterials

journal homepage: www.elsevier.com/locate/biomaterials

Injectable stem cell-laden supramolecular hydrogels enhance in situ osteochondral regeneration via the sustained co-delivery of hydrophilic and hydrophobic chondrogenic molecules

Jianbin Xu[a,1], Qian Feng[b,1], Sien Lin[c,1], Weihao Yuan[d], Rui Li[d], Jinming Li[d,e], Kongchang Wei[d,f], Xiaoyu Chen[d], Kunyu Zhang[d], Yanhua Yang[g], Tianyi Wu[g], Bin Wang[g], Meiling Zhu[g], Rui Guo[h], Gang Li[g,**], Liming Bian[d,i,j,*]

[a] Sir Run Run Shaw Hospital, School of Medicine, Zhejiang University, Hangzhou, Zhejiang, 310016, PR China
[b] Fujian Provincial Key Laboratory of Advanced Materials Oriented Chemical Engineering, College of Chemistry and Materials Science, Fujian Normal University, Fuzhou, 350007, PR China
[c] Orthopaedic Center, Affiliated Hospital of Guangdong Medical University, Zhanjiang, Guangdong, 524001, PR China
[d] Department of Biomedical Engineering, The Chinese University of Hong Kong, Shatin, New Territories, 999077, Hong Kong, China
[e] MOE Key Laboratory of Laser Life Science & Institute of Laser Life Science, College of Biophotonics, South China Normal University, Guangzhou, 510631, PR China
[f] Empa, Swiss Federal Laboratories for Materials Science and Technology, Laboratory for Biomimetic Membranes and Textiles, Lerchenfeldstrasse 5, CH-9014 St. Gallen, Switzerland
[g] Department of Orthopaedics and Traumatology, Faculty of Medicine, The Chinese University of Hong Kong, Shatin, New Territories, 999077, Hong Kong, China
[h] Key Laboratory of Biomaterials of Guangdong Higher Education Institutes, Guangdong Provincial Engineering and Technological Research Center for Drug Carrier Development, Department of Biomedical Engineering, Jinan University, Guangzhou, 510632, PR China
[i] Shenzhen Research Institute, The Chinese University of Hong Kong, Shenzhen, 518172, PR China
[j] Center for Novel Biomaterials, The Chinese University of Hong Kong, Shatin, New Territories, 999077, Hong Kong, China

ARTICLE INFO

Keywords:
Cartilage repair
HGM hydrogel
Drug delivery
Mesenchymal stem cells
Chondrogenic differentiation

ABSTRACT

Hydrogels have been widely used as the carrier material of therapeutic cell and drugs for articular cartilage repair. We previously demonstrated a unique host-guest macromer (HGM) approach to prepare mechanically resilient, self-healing and injectable supramolecular gelatin hydrogels free of chemical crosslinking. In this work, we show that compared with conventional hydrogels our supramolecular gelatin hydrogels mediate more sustained release of small molecular (kartogenin) and proteinaceous (TGF-β1) chondrogenic agents, leading to enhanced chondrogenesis of the encapsulated human bone marrow-derived mesenchymal stem cells (hBMSCs) *in vitro* and *in vivo*. More importantly, the supramolecular nature of our hydrogels allows injection of the pre-fabricated hydrogels containing the encapsulated hBMSCs and chondrogenic agents, and our data show that the injection process has little negative impact on the viability and chondrogenesis of the encapsulated cells and subsequent neocartilage development. Furthermore, the stem cell-laden supramolecular hydrogels administered via injection through a needle effectively promote the regeneration of both hyaline cartilage and subchondral bone in the rat osteochondral defect model. These results demonstrate that our supramolecular HGM hydrogels are promising delivery biomaterials of therapeutic agents and cells for cartilage repair via minimally invasive procedures. This unique capability of injecting cell-laden hydrogels to target sites will greatly facilitate stem cell therapies.

1. Introduction

Articular cartilage has limited self-repair capacity, and the degeneration of articular cartilage leads to osteoarthritis, a severely debilitating disease [1]. Human bone marrow-derived mesenchymal stem cells (hBMSCs) have become increasingly popular as a cell source

* Corresponding author. Department of Biomedical Engineering, The Chinese University of Hong Kong, Shatin, New Territories, Hong Kong, China.
** Corresponding author. Department of Orthopaedics and Traumatology, Faculty of Medicine, The Chinese University of Hong Kong, Shatin, New Territories, Hong Kong, China.
E-mail addresses: gangli@cuhk.edu.hk (G. Li), lbian@cuhk.edu.hk (L. Bian).
[1] Equal contributed to this work.

https://doi.org/10.1016/j.biomaterials.2019.04.031
Received 20 January 2019; Received in revised form 22 April 2019; Accepted 26 April 2019
Available online 28 April 2019
0142-9612/

for repairing cartilage due to their multipotency and easy availability [2]. However, direct administrations of hBMSCs into cartilage defects often lead to limited cartilage regeneration due to significant cell loss and death as a result of the harsh mechanical loading and catabolic factors in the diseased joints [3]. The lack of a functional carrier material to provide physical protection and biochemical cues to the delivered cells in the cartilage defects results in poor retention, significant death and unsatisfactory differentiation of the cells [4]. Therefore, there exists a huge demand for effective carrier biomaterials that afford not only physical support but also biochemical signals to the delivered cells in order to promote the cartilage repair.

A variety of natural and synthetic materials have been used as potential carrier biomaterials of cell or therapeutic agents for cartilage repair [5]. Hydrogels made of various polymers have been shown to promote the chondrogenesis of hBMSCs and cartilage regeneration in the presence of inductive factors by providing the conducive 3D microenvironment [6,7]. Previous studies have demonstrated that the success of hydrogels as the scaffold for regenerative therapies is not only dependent on the proper functioning of the implant material itself but also on the restoration of the overall defect environment [8]. However, most of these hydrogels that allow cell encapsulation are brittle and lack the capability of self-healing and being injectable [9]. Therefore, these hydrogels have high risk of failure once implanted at the load bearing cartilage sites and afford little physical protection to the encapsulated cells [10]. Furthermore, the lack of injectability of these hydrogels precludes the delivery via a minimally invasive procedure, which becomes increasingly popular due to the demand for aesthetic appearance and expeditious post-surgery recovery [11].

In addition to the physical support provided by the biomaterial scaffold, the successful chondrogenesis of hBMSCs and regeneration of cartilage also requires a sustained exposure of the hBMSCs to chondrogenic factors including small molecules and growth factors [12]. However, many chondrogenic small molecules are hydrophobic and have low water solubility, which makes the efficient loading of such small molecules in the highly hydrophilic hydrogel network very challenging [13]. Moreover, although the proteinaceous growth factors can be easily encapsulated into hydrogels, their releases from the cell-laden hydrogels are usually precipitous due to the porous hydrogel network that is necessary for the survival of the seeded cells [14]. Therefore, to facilitate the clinical translation of the hBMSCs in cartilage regeneration, there exists an acute demand on functional hydrogels that not only afford adequate physical protection and facile delivery minimal-invasively but also provide long-term exposure of chondrogenic factors to the encapsulated hBMSCs.

In our previous study, we demonstrated the fabrication of a unique gelatin supramolecular hydrogel via a novel “Host-Guest Macromer” (HGM) approach, which is free from chemical modifications and direct crosslinking of the biopolymers [15] (Fig. 1). The obtained hydrogels (referred to as the “HGM hydrogels” afterwards) are stabilized by the host-guest interaction between the oligomerized Ac-β-CDs and the aromatic residues of gelatin. Such gelatin HGM hydrogels show enhanced physical and biological functionalities including self-healing, mechanical resilience, injectability under the gelation state, shape adapting, controlled release of hydrophobic small molecule drugs, and supporting cell infiltration [15]. These unique features of our gelatin HGM hydrogels well address the aforementioned demands on the effective biomaterial carrier for the delivery of hBMSCs to aid cartilage regeneration.

In this work, we evaluated the gelatin HGM hydrogels for the long-term chondrogenesis of hBMSCs under both the *in vitro* and *in vivo* condition. The hydrophobic cavity of the excess uncomplexed β-CDs in the HGM hydrogels allow the efficient loading and the subsequent sustained release of the hydrophobic drug kartogenin (KGN), thereby promoting the chondrogenesis of the encapsulated hBMSCs (Fig. 1). Moreover, the weak host-guest crosslink formed by the complexation between Ac-β-CDs and the aromatic residues of gelatin affords the gelatin HGM hydrogels with excellent injectability even under gelation state [15]. Therefore, our HGM hydrogels can be prepared with the encapsulated cells and drugs first, stored in the cluture condition, and injected into the recipients at a prescribed time via a minimally invasive procedure (Fig. 2). We demonstrate that the HGM hydrogels enhance the chondrogenesis of the encapsulated hBMSCs compared to the conventional chemically crosslinked gelatin hydrogels of the identical gelatin content both *in vitro* and *in vivo*. Furthermore, the stem cell-laden HGM hydrogels administered via injection effectively promote the regeneration of hyaline cartilage and subchondral bone in the rat osteochondral defect model. The unique properties of our HGM supramolecular hydrogels make them ideal carrier materials of therapeutic cells/drugs for cartilage repair via minimally invasive procedures.

2. Materials and methods

2.1. Acrylate β-cyclodextrin (Ac-β-CD) preparation

10 g β-CDs were dissolved in 150 mL DMF with the addtion of 7 mL TEA, and then the mixture was stirred and cooled down to 0 °C before 5 ml Acryloyl chloride was added into the reaction mixture. After stirring for 12 h, the mixture was filtrated to remove trimethylamine hydrochloride and the obtained clear solution was concentrated to about 10 ml by vacuum rotary evaporation. Then the solution was dripped into 600 ml acetone to precipitate the modified β-CD. The precipitate was washed several times with acetone and vacuum dried for 3 days. The substitution degree (DS) was confirmed to be one single acrylate per β-CD by ^{1}H NMR (Bruker Advance 400 MHz spectrometer). It was recorded in DMSO-d_6 with DMMA as the internal reference at 37 °C [15].

2.2. Methacrylated gelatin (GelMA) preparation

10 g gelatin (type A) was dissolved in 100 mL PBS at 50 °C. A total of 12 mL methacrylic anhydride was then added to the 10% (w/v) gelatin solution and stirred for 4 h at 50 °C. The resulting mixture was dialyzed against deionized water (DI water) for one week at 45 °C to remove the unreacted reagent (6 KDa cut-off dialysis membranes). Then, the obtained product was lyophilized for 4 days at −104 °C. The degree of methacrylation was determined to be 3.17×10^{-4} mol of methacryate groups per gram of gelatin by ^{1}H NMR (Bruker Advance 400 MHz spectrometer). It was recorded in Deuterium oxide (D_2O) with dimethylmaleic anhydride (DMMA) as the internal reference at 37 °C [16].

2.3. HGM supramolecular gelatin hydrogel

Gelatin is physically coupled to mobile acrylated β-cyclodextrins (Ac-β-CDs) via the host-guest interaction between the Ac-β-CDs and the aromatic residues of gelatin to obtain the HGM. Subsequent UV-initiated oligomerization of the acrylate groups of Ac-β-CDs produces the gelatin HGM supramolecular hydrogels. Briefly, gelatin and Ac-β-CDs were dissolved in PBS at 37 °C to produce mixture solutions with the fixed concentration of 8% (w/v) gelatin and f 10% (w/v) Ac-β-CD. Then initiator I2959 was added at 0.05% (w/v). The mixture was pipetted into PVC molds at 37 °C, cooled down to 25 °C, and then exposed to 365 nm ultraviolet (UV) light (10 mW/cm^2, 10 min) at 25 °C to form supramolecular hydrogels. The PVC molds were cylinder-shaped with 5 mm diameter and 3 mm depth [15].

2.4. GelMA hydrogel

8% (w/v) of methacrylated gelatin and 0.05% (w/v) of I2959 were dissolved in PBS at 37 °C. The solution was pipetted into PVC molds and cooled down to 25 °C before exposed to 365 nm UV light (10 mW/cm^2, 10 min) at 25 °C to obtain the chemically crosslinked methacrylated

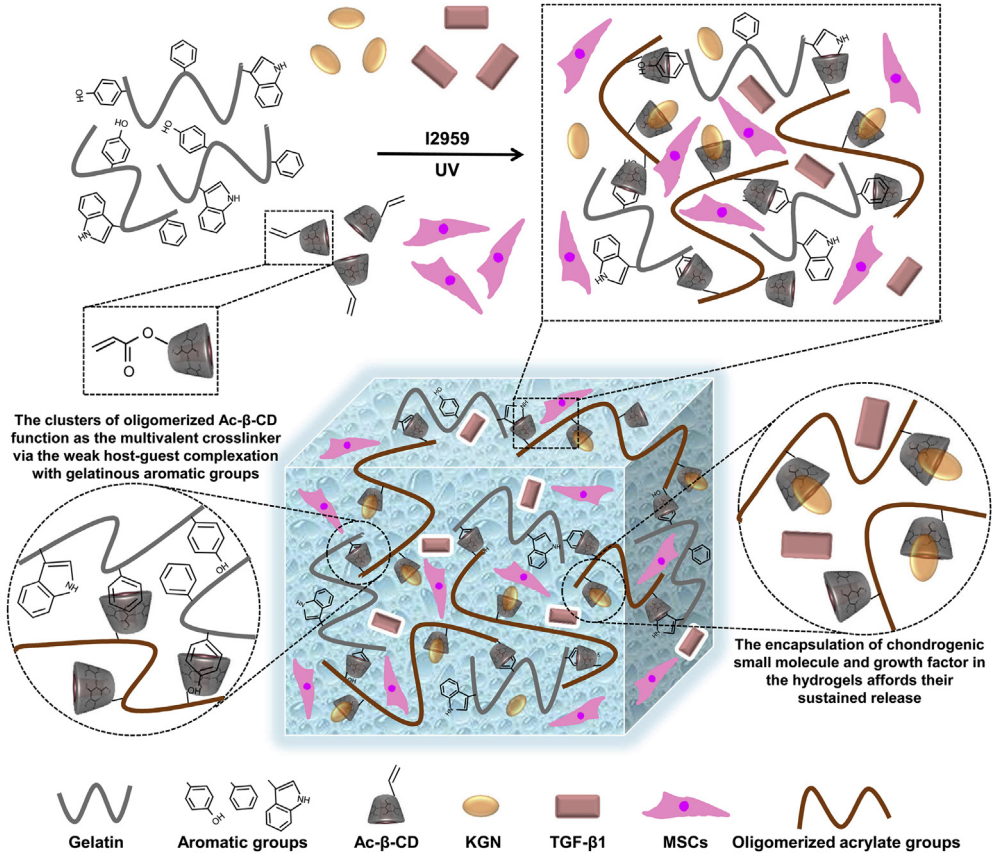

Fig. 1. Schematic illustration of the encapsulation of MSCs, chondrogenic small molecules, and growth factors in the injectable gelatin HGM supramolecular hydrogels.

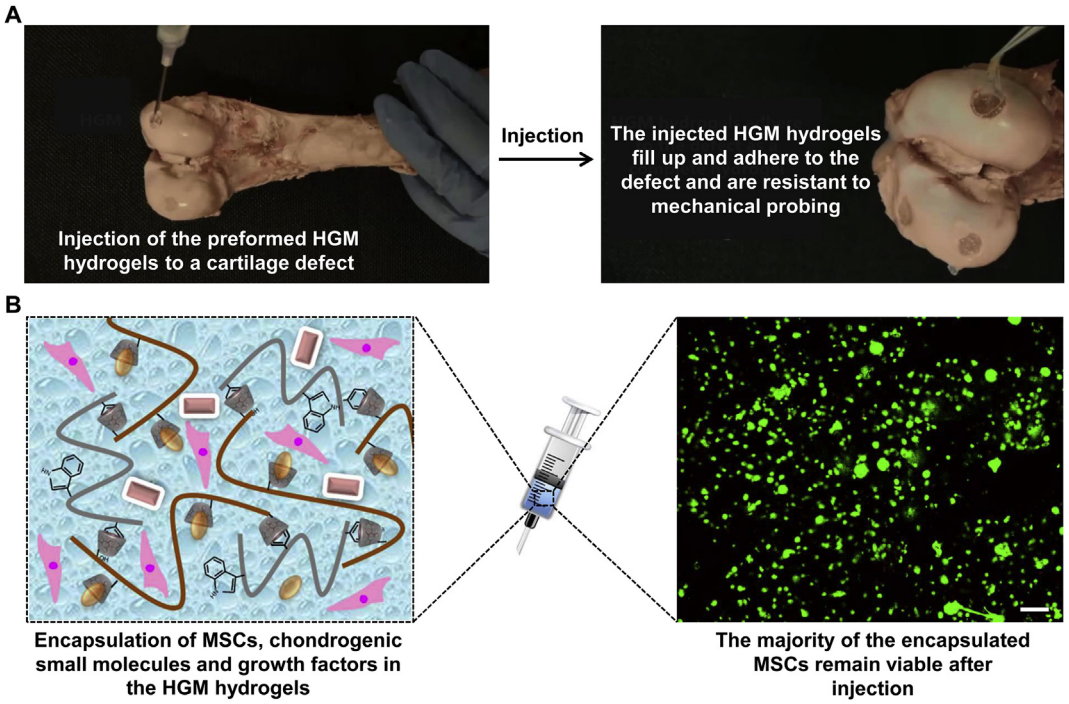

Fig. 2. The injection of HGM gelatin supramolecular hydrogels that are encapsulated with MSCs, chondrogenic small molecules and growth factors for cartilage repair. (A) The injection of pre-formed gelatin HGM supramolecular hydrogels to adhere the cartilage defect. (B) The viability of hBMSCs in pre-formed gelatin HGM supramolecular hydrogels after injection via a G18 needle superimposed image of both calcein-AM (green, live) and ethidium bromide (red, dead) staining. Scale bar: 100 μm. (For interpretation of the references to colour in this figure legend, the reader is referred to the Web version of this article.)

gelatin hydrogel, named GelMA [16].

2.5. Analysis of the release behavior of encapsulated KGN or BSA from hydrogels in vitro

KGN or BSA was mixed with the pre-gelation solution of HGM or GelMA hydrogels for hydrogel preparation in 5 mm diameter x 3 mm thickness PVC molds, respectively, before the gelation. The as-prepared hydrogels were then immersed in 1 mL PBS. 50 μL PBS from each sample was collected from the supernatant at 1 day, 3 day, 5 day, 7 day, 14 day, 21 day, and 28 day to analyze the amount of released KGN or BSA. KGN content was determined by UV–Vis spectrophotometer (absorbance at 205 nm), and the BSA content was quantified by BCA protein quantification kit to calculate the percentage of releasing KGN or BSA.

2.6. Hydrogel swelling analysis

To evaluated the swelling, the freshly prepared GelMA and HGM hydrogels (200 μL per gel, n = 5) were incubated free floating at 37 °C in PBS for 24 h after the measurement of volume (V1). Then, the samples were blotted to remove the residual surface liquid, and the swollen volume (V2) was recorded. The volume swelling ratio was then calculated as the ratio of V2 to V1.

2.7. In vitro culture of hMSC-laden hydrogels

hBMSCs (Lonza, Walkersville, Maryland, USA) were expanded to passage 3 by using growth medium consisting of α-minimum essential medium with 16.7% fetal bovine serum, 1% penicillin/streptomycin and 1% L-glutamine. For three-dimensional (3D) culture, 1% (w/v) PEGDA was added during the fabrication of the hMSC-laden HGM supramolecular gelatin hydrogels in order to prolong the stability of the HGM hydrogels for long term culture (n = 10 for each group). The addition of the PEGDA at this low concentration did not significantly alter the unique features of the HGM hydrogels (Fig. S1). 1×10^7/mL hBMSCs were then photoencapsulated into HGM or GelMA hydrogels with the exposure of UV (365 nm, 10 mW/cm^2, 5 min). TGF-β1 solution was directly mixed with the pre-gelation solution of HGM or GelMA hydrogels before gelation to form the hydrogels in molds, and this is similar as the protocol used for loading BSA in the hydrogel for release kinetics study. The viability of the encapsulated cells was examined by the calcein AM (Live) and ethidium bromide (Dead) staining.

2.8. Gene expression analysis

For gene expression analysis, samples were homogenized in Trizol reagent (Invitrogen), RNA was extracted according to the manufacturer's instructions, and the RNA concentration was determined using an ND-1000 spectrophotometer (Nanodrop Technologies). One microgram of RNA from each sample was reverse-transcribed into cDNA using reverse transcriptase and oligoDT (Thermo). Real-time PCR was performed on an Applied Biosystems 7300 Real-Time PCR system using Taqman primers and probes specific for GAPDH (housekeeping gene) and other genes of interest. Sequences of the primers and probes used are listed in Table S1. The relative gene expression was calculated using the ΔΔCT method, where fold difference was calculated using the expression 2ΔΔCt.

2.9. Subcutaneous implantation of hydrogel in nude mice

All animal experiments in this study were performed in accordance with Animal (Control of Experiments) Ordinance of Hong Kong SAR. And the research protocols were also approved by the Animal Experimentation Ethics Committee (AEEC) of the Chinese University of Hong Kong (AEEC No.: 12-022-MIS1). Animals were housing in local authentic vivarium conditions at temperature of 25–26 °C and a humidity of 70% with free access to water and a pelleted commercial diet. Four different groups (HGM with KGN, HGM with TGF-β1, GelMA with KGN and GelMA with TGF-β1 groups) of hMSCs-laden HGM and GelMA hydrogels (n = 4 for each group) loaded with either KGN or TGF-β1 were implanted into the subcutaneous pockets on the back of male nude mice aging 10-week old were anesthetized with ketamine and xylazine (4 pockets for every nude mouse). For the injection group, HGM hydrogels (n = 4 for each group) with KGN and TGF-β1 were injected into the back of nude mice subcutaneously through a G18 needle. After 28 days of implantation, all the nude mice survived until sacrificed by overdose of pentobarbital. The harvested samples were fixed by 4% paraformaldehyde for analysis.

2.10. Histological analysis in vitro and in vivo

The constructs were fixed in 4% formalin for 24 h, embedded in paraffin and processed using standard histological procedures. The histological sections (7 μm thick) were stained for targets of interest using the Vectastain ABC kit and the DAB Substrate kit for peroxidase (Vector Labs). Briefly, sections were predigested in 0.5 mg mL^{-1} hyaluronidase for 30 min at 37 °C and incubated in 0.5 N acetic acid for 4 h at 4 °C to swell the samples prior to overnight incubation with primary antibodies at dilutions of 1:3 and 1:200 for Collagen II (mouse monoclonal anti-collagen type II, Developmental Studies Hybridoma Bank) and CS (mouse monoclonal anti-chondroitin sulphate, Sigma), respectively.

2.11. Biochemical analysis

The glycosaminoglycan (GAG) content was measured using the dimethylmethylene blue (DMMB; Sigma Chemicals) dye-binding assay with shark chondroitin sulphate (0–50 mg mL^{-1}) as a standard.

2.12. Implantation in rat knee osteochondral defects

As mentioned above, the animal experiments were performed in accordance with the Animal (Control of Experiments) Ordinance of Hong Kong SAR and AEEC of the Chinese University of Hong Kong (AEEC No.: 12-022-MIS1). And the animals were also housing in an authentic animal facility. Briefly, 4 months old SD rat (n = 50) were anesthetized with katamine and xylazine and the right knee joints were exposed through a medial parapatellar approach after shaving and disinfection. The patella was dislocated laterally and the knee placed in full flexion. Then a defect (Ø2 mm, and 5 mm in depth) was created in the center of the groove, using a dental drill. All debris was removed from the defect with a curette and irrigation. Depending on the experimental group, the defect was either treated with PBS as the negative control or repaired by using the following hydrogels loaded with chondrogenic agents: GelMA with KGN, GelMA with TGF-β1, HGM (Injection) with KGN, and HGM (Injection) with TGF-β1. Rat MSCs (rMSCs) were encapsulated in all hydrogel treatment groups at a seeding density of 1×10^7/mL. For the HGM groups, cell-laden HGM hydrogels were injected to the defect via a G18 needle. For the GelMA groups, cell-laden GelMA hydrogels were press fit into the defect. The patella was restored, and the joint capsule, subcutaneous tissue and skin was closed with sutures. All the animals survived until endpoint sacrifice. Right femur was collected under anesthesia by over dose of pentobarbital after 6 weeks of implantation. Left femur was collected as the intact control. Femoral samples were fixed in 10% buffered formalin then decalcified in 10% buffered EDTA (Sigma-Aldrich, St. Louis, MO).

2.13. Cartilage repair analysis by the Wakitani scoring system

The decalcified femoral samples (n = 10 per group) were fixed in 4% formalin for 24 h, embedded in paraffin and processed using

standard histological procedures. 5 μm thick sections were prepared by Leica 2155 microtome (Leica, Wetzlar, Germany), then followed with Safranin O & Fast Green (both from Sigma-Aldrich, St. Louis, MO) stain. Histological sections from the lateral and medial regions of each defect (total of 16 or 20 images per group) were blindly scored by three independent researchers based on a previously established scoring system [17]. Sections were scored for the extent of cartilage repair based on 5 criteria, as shown in Table S2.

2.14. Statistical analysis

All the quantitative data were presented as mean ± standard deviation (SD). After checking of normal distribution by Kolmogorov-Smirnov test, all parameters were analyzed by two-way ANOVA and post hoc Turkey's HSD. For histological analysis, non-parametric Mann-Whitney U tests were used for comparisons between groups. The statistical analysis was calculated by SPSS (version 16; SPSS Inc, Chicago, IL). *: $p < 0.05$, **: $p < 0.01$, ***: $p < 0.001$.

3. Results and discussion

3.1. HGM hydrogels maintain the viability of the encapsulated hBMSCs

The pre-formed HGM hydrogels can be injected by hand to completely fill up the cartilage defect volume, and the injected HGM hydrogels adhere to the surrounding cartilage and remain in position under mechanical probing by a tweezer (Articular cartilage and bone shown in the image are from pigs) (Fig. 2A and Video 1). We injected the pre-formed hMSC-laden gelatin HGM supramolecular hydrogels via a G18 needle, and the viability staining of the injected hydrogels after 3 days of culture shows that majority of the encapsulated cells survive the injection process and remain viable (Fig. 2B). We further evaluated the viability of the hBMSCs encapsulated in the gelatin HGM hydrogels and the control GelMA hydrogels during extended *in vitro* culture. After 14 days of chondrogenic culture, the majority (> 95%) of the hBMSCs encapsulated in the GelMA and HGM hydrogels remain viable (Fig. S2). Interestingly, the hBMSCs encapsulated in the HGM hydrogels show substantial spreading after 14 days of culture, whereas the hBMSCs in the GelMA hydrogels remain the initial rounded morphology (Fig. 3A). This finding indicates that the cells encapsulated in the HGM hydrogels are able to actively interact with the surrounding hydrogel structures.

Supplementary video related to this article can be found at https://doi.org/10.1016/j.biomaterials.2019.04.031.

The weak and reversible host-guest physical crosslinking in the HGM hydrogels likely allows the clustering of the integrin receptors binding to the ligating domains in gelatin, thereby leading to such extensive cell-matrix interactions [15]. In contrast, the non-degradable covalent crosslinking in the GelMA hydrogels inhibits such aggregation of the integrin receptors, thereby limiting the extent of cell-matrix interaction [18]. Mature chondrocytes are known for the rounded morphology. However, the differentiating hBMSCs with spread morphology in the HGM hydrogels actually express significantly higher level of chondrogenic marker gene and produce more cartilaginous matrix [19,20]. This may be attributed to the enhanced cell-cell interactions, which is known to promote the chondrogenesis, in the HGM hydrogels due to the cell spreading enabled by the physical crosslinking of the HGM hydrogels.

The chondrogenic differentiation of MSCs in hydrogels requires the hydrogels to provide a conducive 3D microenvironment [21]. For example, cell–cell contact via membranous molecules such as N-cadherin is known to be critical to the chondrogenesis of MSCs [22]. However, most of the conventional chemically-crosslinked hydrogels with high crosslink density restrict such cell-cell contacts due to the slow-degrading and statically-crosslinked network structure [23]. We previously showed that conjugating the N-cadherin peptide in such static hydrogels can enhance the chondrogenesis of encapsulated MSCs by mimicking the N-cadherin-mediated cell-cell contact and inhibiting the canonical Wnt signaling as evidenced by the results from PCR, Western blot and gene microarray analysis [24,25]. Moreover, our previous work also showed that our injectable supramolecular hydrogels better support the spreading of encapsualted MSCs due to the dynamic and reversible crosslinks in the hydrogel network, and such permissive 3D microenvironment potentially faciliates cell-cell contact and subsequent chondrognesis of MSCs in the presence of chondrogenic inductive factors.

3.2. HGM hydrogels mediate prolonged release of encapsulated hydrophobic drug KGN and a model protein

We further encapsulated a hydrophobic chondrogenic small molecule, kartogenin (KGN), or a model protein, bovine serum albumin (BSA), in the HGM hydrogels to assess the *in vitro* release kinetics. Our finding shows that the release profiles of the cargo molecules from the HGM hydrogel are significantly different from those of the GelMA hydrogels (KGN: $p < 0.01$, BSA: $p < 0.05$). The HGM hydrogels release the loaded KGN continuously for up to 28 days at an almost constant rate (Fig. 3B). In contrast, almost all the loaded KGN is rapidly released out from the GelMA hydrogels within 7 days. Unlike most of the traditional hydrogels that are not able to retain hydrophobic small molecules because of the hydrophilic structure, our HGM hydrogels can hold hydrophobic small molecular drugs in the unoccupied hydrophobic β-CD cavities [26,27]. It should be noted that cyclodextrins have long been used in the pharmaceutical industry to improve the solubility and bioavailability of hydrophobic drugs [28]. At the same time, the HGM hydrogels release the encapsulated BSA more slowly than the GelMA hydrogels (Fig. 3C). We speculate that the nanodomains of the host-

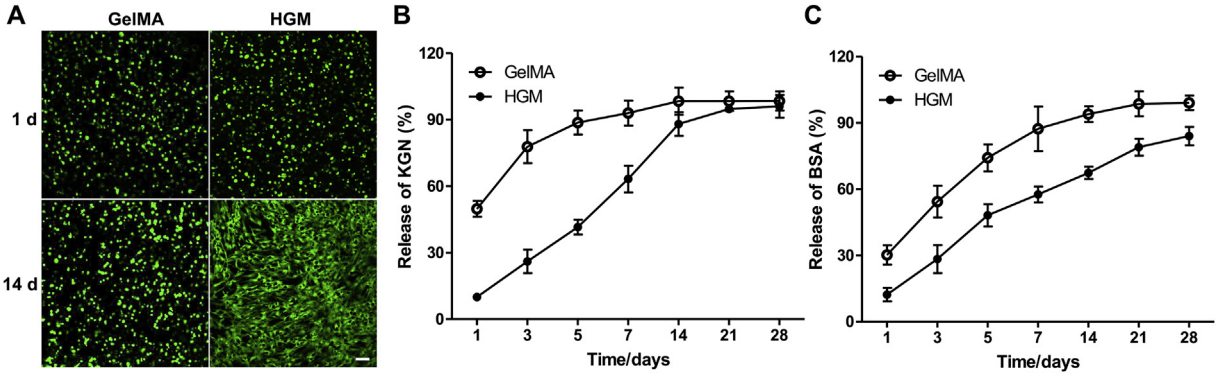

Fig. 3. (A) Cell viability staining of the hMSC-laden GelMA and HGM hydrogels after 1 day and 14 days of culture superimposed image of both calcein-AM (green, live) and ethidium bromide (red, dead) staining. Cumulative release of KGN (B) and BSA (C) encapsulated in the GelMA and HGM hydrogels. Scale bar: 100 μm. (For interpretation of the references to colour in this figure legend, the reader is referred to the Web version of this article.)

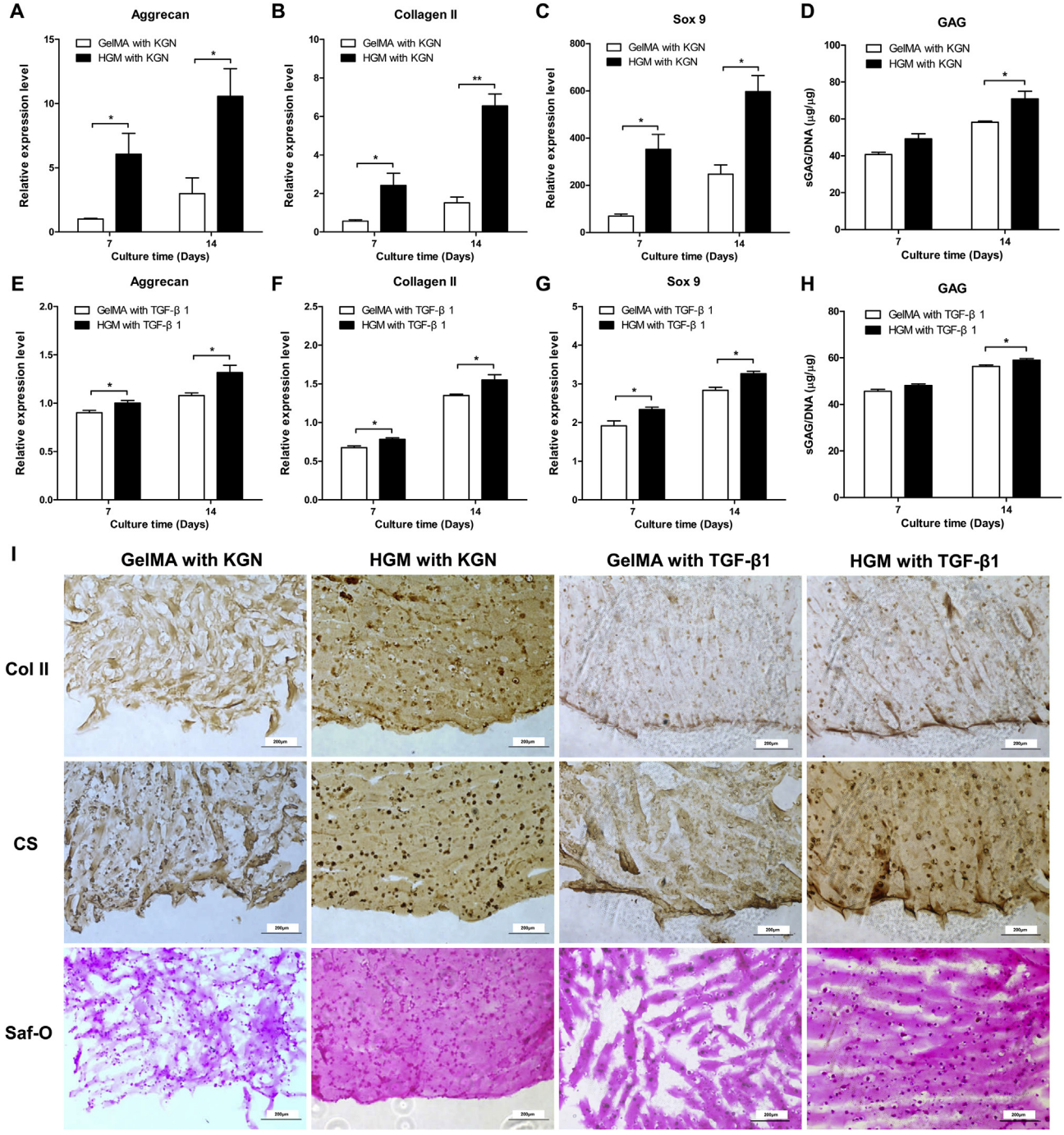

Fig. 4. The chondrogenic differentiation of hBMSCs in the HGM hydrogels loading with KGN or TGF-β1 *in vitro*. The mRNA expression of chondrogenic marker genes of hBMSCs-laden GelMA and HGM hydrogels constructs with KGN and TGF-β1. Relative gene expression of Aggrecan (A, E), type II Collagen (B, F), and Sox 9 (C, G) by the hBMSCs after 7 and 14 days of differentiation is presented. GAG content of hBMSCs-laden GelMA and HGM hydrogels constructs with KGN and TGF-β1. Comparison of GAG content in chondrogenic differentiation medium supplemented with KGN (D) and TGF-β1 (H) at 7 days and 14 days. (I) Immunohistochemical and histological staining of hMSC-laden hydrogels with KGN and TGF-β1 after 14 days chondrogenic differentiation. Immunohistochemical and histological staining of type II Collagen (col II), Chondroitin sulphate (CS) and Safranin-O (Saf-O) of hBMSCs-laden hydrogels, respectively. The data are reported as the mean ± SD of the experiments (n = 3). *: $p < 0.05$, **: $p < 0.01$. Scale bar indicates 200 μm.

guest clusters in the HGM hydrogels, which may function as nanovessels to harbor the BSA molecules, contribute to the improved retention of the BSA molecules within the HGM hydrogels [29,30]. These results indicate that the HGM hydrogels afford enhanced storage and sustained release of the KGN and TGF-β1, which will promote the chondrogenesis of the encapsulated hBMSCs. Furthermore, these *in vitro* studies suggest that the HGM hydrogels are more promising than the GelMA hydrogels as the delivery vehicles of chondrogenic agents for cartilage regeneration under the *in vivo* condition, where a sustained release of an initial bolus dosage of these agents is desired.

3.3. HGM hydrogels enhance the chondrogenic differentiation of encapsulated hBMSCs in vitro

We evaluated the chondrogenesis of hBMSCs in the KGN (0.5 nmol per hydrogel) or TGF-β1-laden (50 ng per hydrogel) HGM and GelMA

hydrogels. After 14 days of induction, the hBMSCs in the HGM hydrogels exhibits significantly higher expression of chondrogenic markers than those in the GelMA hydrogels groups. For the KGN laden hydrogels, the mRNA expression in the HGM with KGN groups is enhanced by about 253.7% ± 178.5%, 332.0% ± 51.5%, and 141.4% ± 69.3% for Aggrecan, type II Collagen, and Sox 9 compared to that of the GelMA with KGN groups at day 14, respectively (Fig. 4A–C). For the TGF-β1 laden hydrogels, the mRNA expression in the HGM with TGF-β1 groups is enhanced by about 22.2% ± 9.4%, 14.9% ± 7.8% and 15.0% ± 8.2% for Aggrecan, type II Collagen, and Sox 9 compared to that of the GelMA with TGF-β1 groups at day 14, respectively (Fig. 4E–G). Consistent with the gene expression results, the quantification of glycosaminoglycans (GAGs), a cartilage-specific matrix component [31], shows that the GAGs content in the HGM group is 21.7% ± 12.3% (loaded with KGN) (Figs. 4D) and 4.7% ± 2.1% (loaded with TGF-β1) (Fig. 4H) higher than that in the GelMA group after 14 days of culture *in vitro*.

Immunohistochemical staining results show that the deposition of type II Collagen (Col II) and chondroitin sulphate (CS), two key components of the cartilage matrix [32], is higher in the HGM hydrogels than in the GelMA hydrogels (Fig. 4I). Moreover, the Safranin-O (Saf-O) staining also support the immunohistochemical staining results, demonstrating more cartilage matrix production by the hBMSCs encapsulated in the HGM hydrogels (Fig. 4I). These results indicate that the sustained exposure of KGN or TGF-β1 in our HGM hydrogels enhances the chondrogenic differentiation of the hBMSCs and the cartilage matrix elaboration.

3.4. HGM hydrogels enhance the chondrogenic differentiation of encapsulated hBMSCs in vivo

We next investigated the chondrogenic differentiation of hBMSCs in the HGM hydrogels loading with KGN or TGF-β1 *in vivo*. We implanted the KGN (1 nmol per hydrogl) or TGF-β1 (100 ng per hydrogel) laden HGM and GelMA hydrogels with the encapsulated hBMSCs into the subcutaneous pockets in nude mice for 28 days (Fig. 5A). Out of the 4 samples implanted per group, 1, 2 and 4 samples were recovered from the "GelMA with KGN", "GelMA with TGF-β1", "HGM with KGN", "HGM with TGF-β1", "HGM (Injection) with KGN" and "HGM (Injection) with TGF-β1" group, respectively. GAG quantification analysis showes that the KGN or TGF-β1 laden HGM groups have 58.8% ± 32.1% and 27.7% ± 11.6% higher GAG contents about compared to the KGN and TGF-β1 laden GelMA group, respectively, after 28 days of the implantation (Fig. 5B).

The immunohistochemical staining reveals more intense staining against type II collagen (Col II) and chondroitin sulphate (CS) in the KGN or TGF-β1 laden HGM hydrogels than that in the KGN or TGF-β1 laden GelMA hydrogels (Fig. 5C). The safranin-O (Saf-O) staining of the histological sections also shows more deposition of proteoglycans in the HGM hydrogels than in the GelMA hydrogels (Fig. 5C). These results incidate that the gelatin HGM hydrogels promote the chondrogenesis of the encapsulated hBMSCs and enhance the neocartilage formation *in vivo*.

To assess the injectability of the HGM hydrogels for *in vivo* applications, we injected the pre-fabricated hBMSCs-laden HGM hydrogels, which were loaded with KGN or TGF-β1, at the gelation state through a 18G needle into the back of nude mice subcutaneously ("HGM (Injection) with KGN/TGF-β1" group). Due to the shear-thinning and self-healing capability, the HGM hydrogels maintain the integral hydrogel structure without fragmentation after the injection and remain so after 28 days of *in vivo* implantation (Fig. 5A). Furthermore, our results showed that after the encapsulation of hMSCs, the cell-laden HGM hydrogels still had good shear-thinning property, and this suggests that the hMSC-laden HGM hydrogels maintain the good injectability (Fig. S3). The maintenance of the monolithic hydrogel structure after implantation is important to the deposition and retention of the cartilaginous matrix produced by the encapsulated cells [33,34].

The GAG quantification, immunohistochemical and histological stainings show that the content of the cartilage-specific matrix components in the KGN/TGF-β1 injected HGM hydrogels ("HGM (injection) with KGN/TGF-β1" group) is significantly higher than that in the KGN/TGF-β1 the GelMA hydrogels ("GelMA with KGN/TGF-β1" group) and are similar to that in the directly implanted (non-injected) HGM hydrogels loaded with the same chondrogenic factor ("HGM with KGN/TGF-β1" group) (Fig. 5). This finding indicates that the injection does not compromise the viability and chondrognesis of the hBMSCs encapsulated in the HGM hydrogels [15,35].

Due to the shear thinning property of the gelatin HGM hydrogels, the HGM hydrogels transform into a "sol" like state under high shear as evidenced by the storage modulus being overtaken by the loss modulus shown in the rheological data (Fig. S4). Therefore, the hBMSCs encapsulated in the HGM hydrogels are likely protected from the excessive shear stress of the injection due to the "sol" transition of the surrounding HGM hydrogels [36,37]. Meanwhile, the swelling ratio of the GelMA and HGM hydrogels showed that HGM hydrogels have higher swelling ratio than GelMA hydrogels (Fig. S5). The excellent injectability of the HGM hydrogels makes them an ideal biomaterial carrier of hBMSCs for cartilage regeneration by minimally invasive procedures.

3.5. HGM hydrogels promote the regeneration of cartilage and subchondral bone in the rat osteochondral defect model

We further assess the efficacy of rMSCs-laden HGM hydrogels loaded with KGN (1 nmol/hydrogel) or TGF-β1 (100 ng per hydrogel) for cartilage regeneration in the osteochondral defects in rat knee. GelMA and HGM hydrogels were pressed fit and injected into the cartilage defects, respectively. 6 weeks after the implantation, as shown in Fig. 6, macroscopic views of defect area reveal fully regenerated cartilage of white and smooth appearance that is well integrated with the surrounding tissue in all the HGM hydrogels groups, closely resembling the healthy control. In contrast, in the GelMA with KGN/TGF-β1 groups, a partial cartilage defect in the center is still clearly visible, and the circular defect boundary is easily distinguishable at the interface with the surrounding health cartilage. In the non-treated (PBS control) group, the defects were almost empty with little regenerated tissue.

Histological examination (Safranin-O and H & E staining) reveals the deposition of disorganized fibrous tissue in the osteochondral defects of the non-treatment group (PBS control) with poor integration to the surrounding native cartilage and no regeneration of subchondral bone (Fig. 7A and B). In the GelMA with KGN/TGF-β1 groups, the defect is filled with a mixture of fibrous and cartilage-like tissue with little regeneration of the subchondral bone. In clear contrast, the defects in the HGM (Injection) with KGN/TGF-β1 groups show more congruent articular surface, enhanced regeneration of cartilage-like tissue and subchondral bone, and organized osteochondral structure, which is similar to that of the healthy control (Fig. 7A and B). The expression of cartilage-specific type II collagen in the defect area is evaluated by immunohistochemical staining (Fig. 7C). Higher levels of type II collagen expression are found in the HGM (Injection) with KGN/TGF-β1 groups than those of the GelMA with KGN/TGF-β1 groups, and these results are consistent to Safranin-O staining results (Fig. 7C).

The quality of the cartilage regeneration is evaluated according to the scoring method described by Wakitani [17,38]. The average Wakitani score is 9.67 ± 1.86 for GelMA with KGN, 9.50 ± 1.52 for GelMA with TGF-β1, 3.83 ± 1.47 for HGM (Injection) with KGN, and 4.50 ± 1.52 for HGM (Injection) with TGF-β1 groups, respectively, 6 weeks after the implantation (Fig. 8). The non-treatment control and healthy control group receives the highest and lowest score, respectively. The HGM (Injection) with KGN/TGF-β1 groups score significantly lower than the GelMA with KGN/TGF-β1 groups, thereby indicating enhanced cartilage regeneration achieved by using the HGM

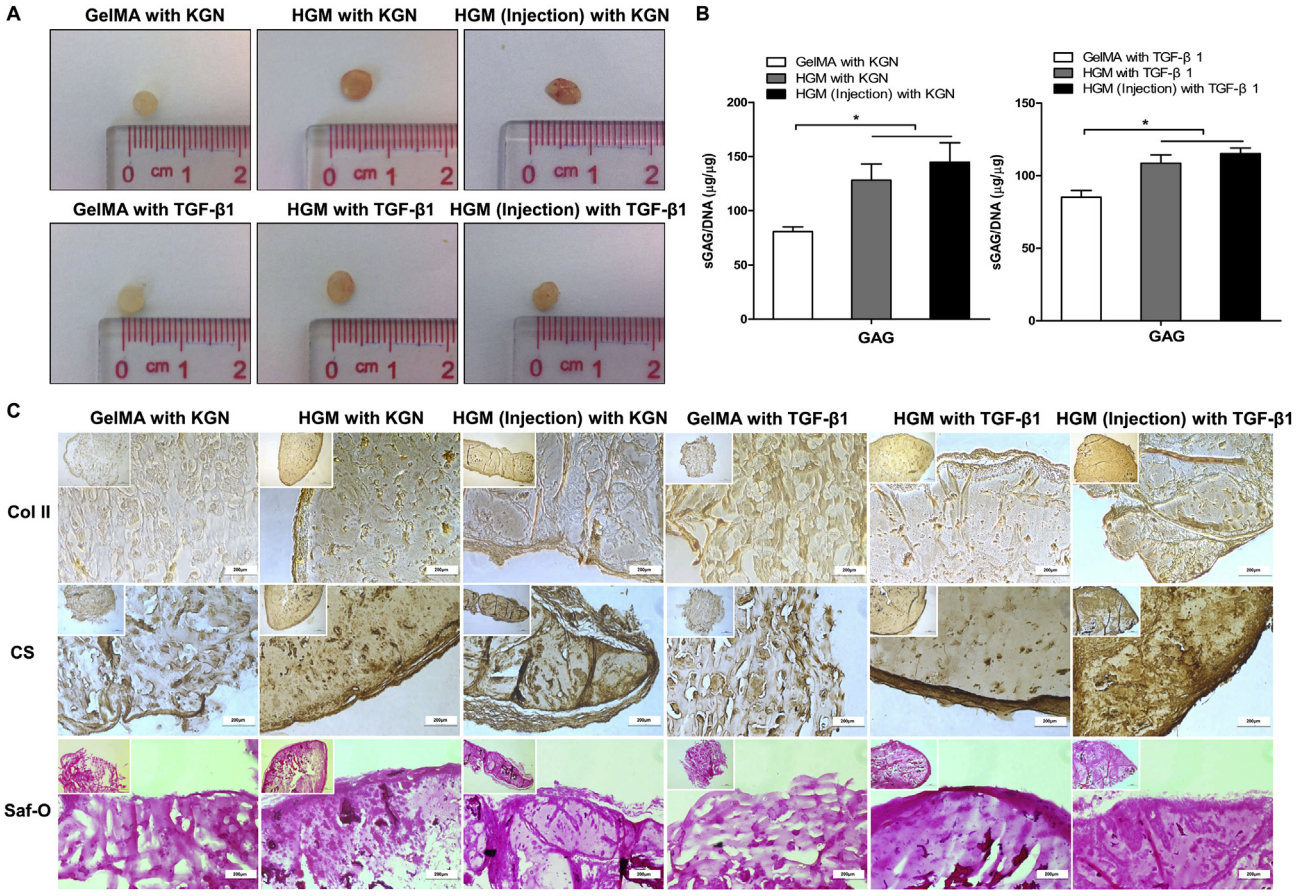

Fig. 5. The chondrogenic differentiation of hBMSCs in the HGM hydrogels loading with KGN or TGF-β1 *in vivo*. Harvested hMSC-laden hydrogel implants after 28 days of subcutaneous implantation in nude mice. (A) Images of the harvested hMSC-laden hydrogel implants with GelMA with KGN, HGM with KGN, HGM (Injection) with KGN, GelMA with TGF-β1, HGM with TGF-β1, and HGM (Injection) with TGF-β1. (B) GAG content of hBMSCs-laden HGM and GelMA hydrogels with KGN and TGF-β1 *in vivo*. (C) Immunohistochemical and histological staining of hMSC-laden hydrogels with KGN and TGF-β1 after 14 days chondrogenic differentiation *in vivo*. Immunohistochemical and histological staining of type II Collagen (col II), Chondroitin sulphate (CS) and Safranin-O (Saf-O) of hBMSCs-laden hydrogels, respectively. The data are reported as the mean ± SD of the experiments (n = 3). *: $p < 0.05$, **: $p < 0.01$. Scale bar indicates 200 μm.

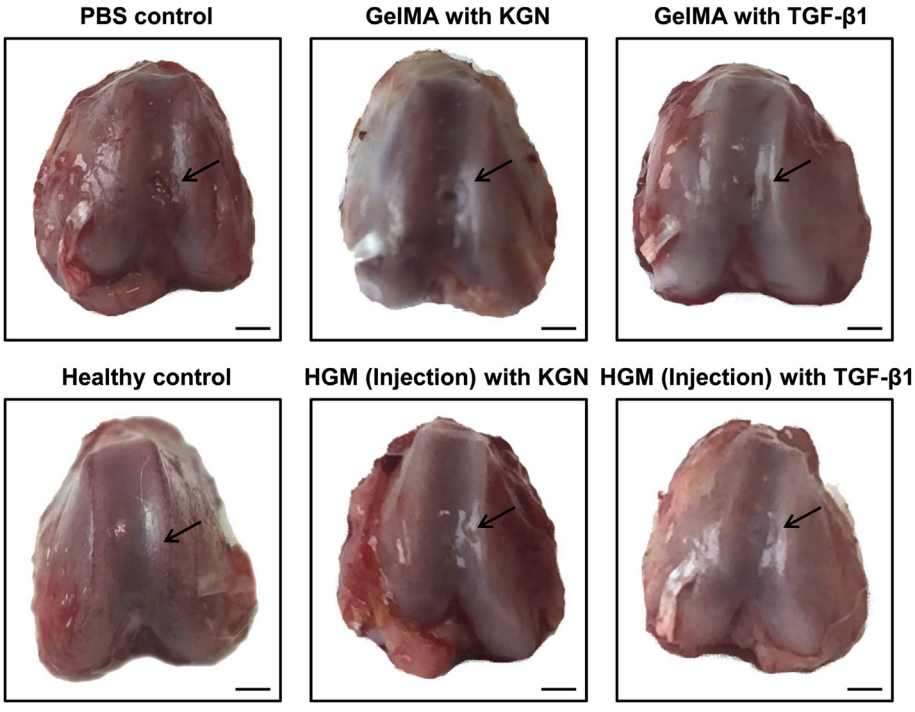

Fig. 6. Macroscopic appearance of the rat knee osteochondral defect either treated with PBS or repaired by using the following hydrogels loaded with chondrogenic agents: GelMA with KGN, HGM (Injection) with KGN, GelMA with TGF-β1, and HGM (Injection) with TGF-β1 at week 6 after surgery. The non-treated (PBS control) and contralateral intact (Healthy control) rat knees were collected as negative controls or health controls, respectively. rMSCs were encapsulated in all hydrogel treatment groups at a seeding density of 1×10^7/mL. Arrow heads point to the location of defects. Scale bar: 2 mm.

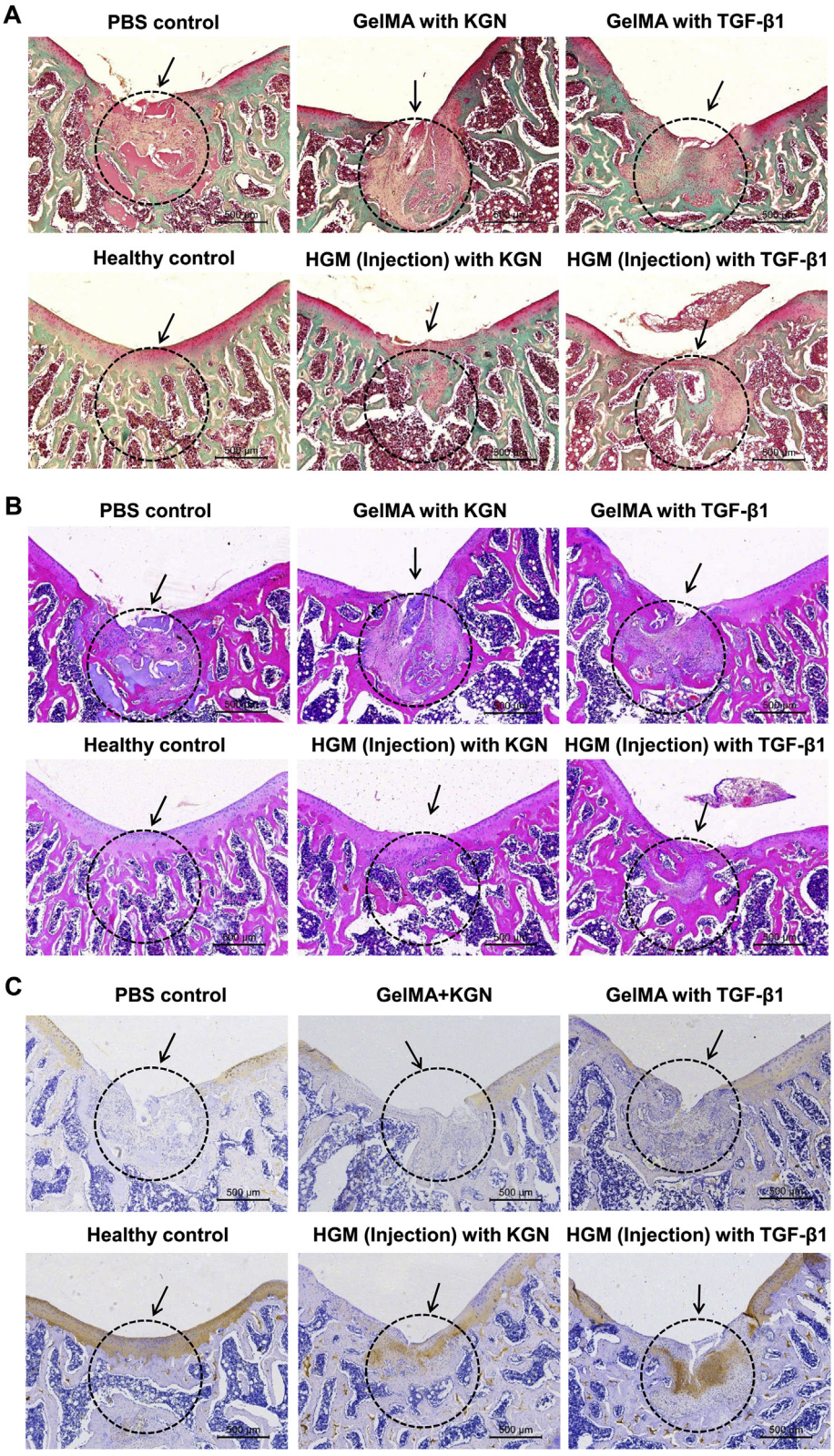

Fig. 7. (A) Safranin-O & fast green staining, (B) H&E staining and (C) immunohistochemical staining against type II collagen of the rat knee osteochondral defects either treated with PBS or repaired by using the following hydrogels loaded with chondrogenic agents: GelMA with KGN, HGM (Injection) with KGN, GelMA with TGF-β1 and HGM (Injection) with TGF-β1 at week 6 after surgery. Arrows heads and dotted circles indicate the location of the articular surface and osteochondral defects, respectively. Scale bar indicates 500 μm. (For interpretation of the references to colour in this figure legend, the reader is referred to the Web version of this article.)

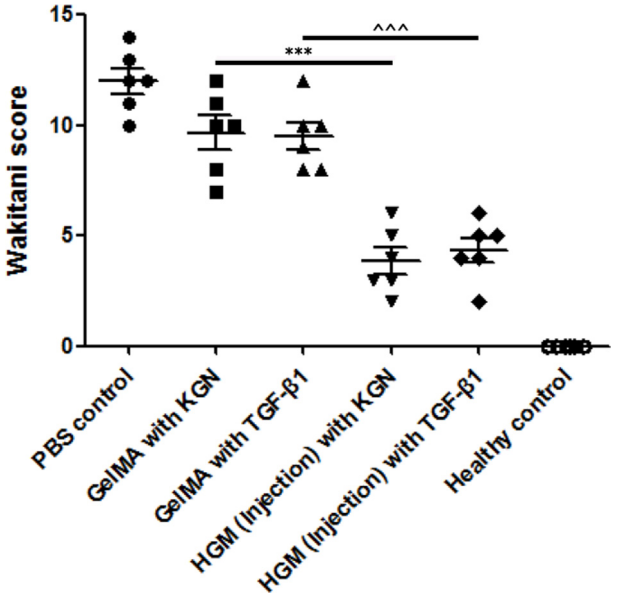

Fig. 8. Cartilage regeneration evaluated by the Wakitani scoring system at week 6 after surgery. $^{***}P < 0.001$ vs. (GelMA with KGN); $^{\wedge\wedge\wedge}P < 0.001$ vs. (GelMA with TGF-β1).

gelatin hydrogels.

These results incidate that the HGM gelatin hydrogels promote the chondrogenesis of the encapsulated rMSCs and enhance the neo-cartilage formation in the rat cartilage defect model. As shown in our earlier works, the HGM hydrogels mediate more prolonged release of hydrophobic small molecules due to the retention effect of β-CDs, and the clustered host-guest complexes in the HGM hydrogels may also improve the retention of the soluble proteins like TGF-β1 within the HGM hydrogels [15,29]. Therefore, the better retentation and therefore sustained release of KGN and TGF-β1 from the HGM hydrogels may contribute to the enhanced chondrogenesis observed in the HGM groups. The enhanced regeneration of subchondral bone observed the HGM groups is likely due to that the weak host-guest crosslink in the HGM hydrogels facilitate the infiltration and migration of endogenous osteoblastic cells from surrounding bone tissues as demonstrated in our previous work [15].

4. Conclusion

Taken together, we demonstrate that the injectable stem cell-laden gelatin supramolecular hydrogels enhance in situ osteochondral regeneration via the sustained co-delivery of hydrophilic and hydrophobic chondrogenic molecules. We demonstrate that the HGM hydrogels enhance the chondrogenesis of the encapsulated hBMSCs under both *in vitro* and *in vivo* condition compared with the conventional chemically crosslinked gelatin hydrogels. Furthermore, the injected MSC-laden HGM hydrogels lead to quality neocartilage formation in the rat knee cartilage defect model, thereby demonstrating the promising potential of the HGM hydrogels as a biomaterial carrier of therapeutic cells and drugs for cartilage regeneration by minimally invasive procedures. Lastly, our findings indicate that our HGM hydrogels can potentially be prepared with the encapsulated cells and drugs first, stored in the culture condition, and injected into the recipients at a prescribed time via a minimally invasive procedure. This unique property of the injectable hydrogel can potentially facilitate the large scale production, distribution, and usage of cell-laden hydrogels.

Conflicts of interest

The authors declare no competing financial interests.

Data availability

The raw/processed data required to reproduce these findings cannot be shared at this time as the data also forms part of an ongoing study.

Acknowledgements

Project is supported by the National Natural Science Foundation of China (No. 31570979 & 81701820). This work is supported by the Science and Technology Project of Guangdong Province (2017A050506011 & 2018A030313374). The work described in this paper is supported by a General Research Fund grant from the Research Grants Council of Hong Kong (Project No. 14202215 & 14220716). This research is supported by an Innovation and Technology Fund (TCFS, GHP/011/17SZ), Hong Kong. The work was partially supported by Hong Kong Research Grants Council Theme-based Research Scheme (Ref. T13-402/17-N). This work is supported by the Health and Medical Research Fund, the Food and Health Bureau, the Government of the Hong Kong Special Administrative Region (reference no.: 03140056). This research is supported by the Chow Yuk Ho Technology Centre for Innovative Medicine, The Chinese University of Hong Kong.

Appendix A. Supplementary data

Supplementary data to this article can be found online at https://doi.org/10.1016/j.biomaterials.2019.04.031.

References

[1] C. Zingler, H.D. Carl, B. Swoboda, S. Krinner, F. Hennig, K. Gelse, Limited evidence of chondrocyte outgrowth from adult human articular cartilage. Osteoarthritis and cartilage/OARS, Osteoarthritis Research Society 24 (2016) 124–128.
[2] C. Madeira, A. Santhagunam, J.B. Salgueiro, J.M. Cabral, Advanced cell therapies for articular cartilage regeneration, Trends Biotechnol. 33 (2015) 35–42.
[3] B.J. Huang, J.C. Hu, K.A. Athanasiou, Cell-based tissue engineering strategies used in the clinical repair of articular cartilage, Biomaterials 98 (2016) 1–22.
[4] G. Ebihara, M. Sato, M. Yamato, G. Mitani, T. Kutsuna, T. Nagai, et al., Cartilage repair in transplanted scaffold-free chondrocyte sheets using a minipig model, Biomaterials 33 (2012) 3846–3851.
[5] Z. Man, X. Hu, Z. Liu, H. Huang, Q. Meng, X. Zhang, et al., Transplantation of allogenic chondrocytes with chitosan hydrogel-demineralized bone matrix hybrid scaffold to repair rabbit cartilage injury, Biomaterials 108 (2016) 157–167.
[6] J. Wang, F. Zhang, W.P. Tsang, C. Wan, C. Wu, Fabrication of injectable high strength hydrogel based on 4-arm star PEG for cartilage tissue engineering, Biomaterials 120 (2017) 11–21.
[7] D. Albani, A. Gloria, C. Giordano, S. Rodilossi, T. Russo, U. D'Amora, et al., Hydrogel-based nanocomposites and mesenchymal stem cells: a promising synergistic strategy for neurodegenerative disorders therapy, Sci. World J. 9 (2013).
[8] S. Reitmaier, A. Shirazi-Adl, M. Bashkuev, H.J. Wilke, A. Gloria, H. Schmidt, In vitro and in silico investigations of disc nucleus replacement, J. R. Soc. Interface 9 (2012) 1869–1879.
[9] J.W. Nichol, S.T. Koshy, H. Bae, C.M. Hwang, S. Yamanlar, A. Khademhosseini, Cell-laden microengineered gelatin methacrylate hydrogels, Biomaterials 31 (2010) 5536–5544.
[10] L.-S. Wang, C. Du, W.S. Toh, A.C.A. Wan, S.J. Gao, M. Kurisawa, Modulation of chondrocyte functions and stiffness-dependent cartilage repair using an injectable enzymatically crosslinked hydrogel with tunable mechanical properties, Biomaterials 35 (2014) 2207–2217.
[11] K. Ren, C. He, C. Xiao, G. Li, X. Chen, Injectable glycopolypeptide hydrogels as biomimetic scaffolds for cartilage tissue engineering, Biomaterials 51 (2015) 238–249.
[12] D. Shi, X. Xu, Y. Ye, K. Song, Y. Cheng, J. Di, et al., Photo-cross-linked scaffold with kartogenin-encapsulated nanoparticles for cartilage regeneration, ACS Nano 10 (2016) 1292–1299.
[13] J. Xu, J. Li, S. Lin, T. Wu, H. Huang, K. Zhang, et al., Nanocarrier-mediated co-delivery of small molecular drugs and siRNA to enhance chondrogenic differentiation and suppress hypertrophy of human mesenchymal stem cells, Adv. Funct. Mater. 26 (2016) 2463–2472.
[14] M. Floren, W. Bonani, A. Dharmarajan, A. Motta, C. Migliaresi, W. Tan, Human mesenchymal stem cells cultured on silk hydrogels with variable stiffness and growth factor differentiate into mature smooth muscle cell phenotype, Acta Biomater. 31 (2016) 156–166.
[15] Q. Feng, K.C. Wei, S.E. Lin, Z. Xu, Y.X. Sun, P. Shi, et al., Mechanically resilient, injectable, and bioadhesive supramolecular gelatin hydrogels crosslinked by weak host-guest interactions assist cell infiltration and in situ tissue regeneration (vol 101, pg 217, 2016), Biomaterials 112 (2017) 346–347.
[16] O. Jeon, D.W. Wolfson, E. Alsberg, In-situ formation of growth-factor-loaded

coacervate microparticle-embedded hydrogels for directing encapsulated stem cell fate, Adv. Mater. 27 (2015) 2216.
[17] S. Wakitani, T. Goto, S.J. Pineda, R.G. Young, J.M. Mansour, A.I. Caplan, et al., Mesenchymal cell-based repair of large, full-thickness defects of articular cartilage, J. Bone Joint Surg. Am. Vol. 76 (1994) 579–592.
[18] S. Khetan, M. Guvendiren, W.R. Legant, D.M. Cohen, C.S. Chen, J.A. Burdick, Degradation-mediated cellular traction directs stem cell fate in covalently cross-linked three-dimensional hydrogels, Nat. Mater. 12 (2013) 458–465.
[19] A.J. Engler, Q. Feng, M. Zhu, K. Wei, L. Bian, Cell-mediated degradation regulates human mesenchymal stem cell chondrogenesis and hypertrophy in MMP-sensitive hyaluronic acid hydrogels, PLoS One 9 (2014) e99587.
[20] X. Xin, M. Hussain, J.J. Mao, Continuing differentiation of human mesenchymal stem cells and induced chondrogenic and osteogenic lineages in electrospun PLGA nanofiber scaffold, Biomaterials 28 (2007) 316–325.
[21] Z.M. Liu, M.L. Tang, J.P. Zhao, R.J. Chai, J.H. Kang, Looking into the future: toward advanced 3D biomaterials for stem-cell-based regenerative medicine, Adv. Mater. 30 (2018) 20.
[22] B.D. Cosgrove, K.L. Mui, T.P. Driscoll, S.R. Caliari, K.D. Mehta, R.K. Assoian, et al., N-cadherin adhesive interactions modulate matrix mechanosensing and fate commitment of mesenchymal stem cells, Nat. Mater. 15 (2016) 1297–1306.
[23] X.Q. Dou, C.L. Feng, Amino acids and peptide-based supramolecular hydrogels for three-dimensional cell culture, Adv. Mater. 29 (2017) 21.
[24] R. Li, J.B. Xu, D.S.H. Wong, J.M. Li, P.C. Zhao, L.M. Bian, Self-assembled N-cadherin mimetic peptide hydrogels promote the chondrogenesis of mesenchymal stem cells through inhibition of canonical Wnt/beta-catenin signaling, Biomaterials 145 (2017) 33–43.
[25] L.M. Bian, M. Guvendiren, R.L. Mauck, J.A. Burdick, Hydrogels that mimic developmentally relevant matrix and N-cadherin interactions enhance MSC chondrogenesis, Proc. Natl. Acad. Sci. U. S. A. 110 (2013) 10117–10122.
[26] M.L. Kang, J.-Y. Ko, J.E. Kim, G.-I. Im, Intra-articular delivery of kartogenin-conjugated chitosan nano/microparticles for cartilage regeneration, Biomaterials 35 (2014) 9984–9994.
[27] C. He, Z. Tang, H. Tian, X. Chen, Co-delivery of chemotherapeutics and proteins for synergistic therapy, Adv. Drug Deliv. Rev. 98 (2016) 64–76.
[28] J. Zhang, K. Ellsworth, P.X. Ma, Hydrophobic pharmaceuticals mediated self-assembly of β-cyclodextrin containing hydrophilic copolymers: novel chemical responsive nano-vehicles for drug delivery, J. Control. Release 145 (2010) 116–123.
[29] K. Wei, M. Zhu, Y. Sun, J. Xu, Q. Feng, S. Lin, et al., Robust biopolymeric supramolecular "Host−Guest macromer" hydrogels reinforced byin SituFormed multivalent nanoclusters for cartilage regeneration, Macromolecules 49 (2016) 866–875.
[30] T. Xie, A. Vora, P.J. Mulcahey, S.E. Nanescu, M. Singh, D.S. Choi, et al., Surface assembly configurations and packing preferences of fibrinogen mediated by the periodicity and alignment control of block copolymer nanodomains, ACS Nano 10 (2016) 7705–7720.
[31] B.V. Sridhar, J.L. Brock, J.S. Silver, J.L. Leight, M.A. Randolph, K.S. Anseth, Development of a cellularly degradable PEG hydrogel to promote articular cartilage extracellular matrix deposition, Adv. Healthc. Mater. 4 (2015) 702–713.
[32] B. Carrion, M.F. Souzanchi, V.T. Wang, G. Tiruchinapally, A. Shikanov, A.J. Putnam, et al., The synergistic effects of matrix stiffness and composition on the response of chondroprogenitor cells in a 3D precondensation microenvironment, Adv. Healthc. Mater. 5 (2016) 1192–1202.
[33] S.J. Bidarra, C.C. Barrias, P.L. Granja, Injectable alginate hydrogels for cell delivery in tissue engineering, Acta Biomater. 10 (2014) 1646–1662.
[34] S. Van Vlierberghe, P. Dubruel, E. Schacht, Biopolymer-based hydrogels as scaffolds for tissue engineering applications: a review, Biomacromolecules 12 (2011) 1387–1408.
[35] H. Park, J.S. Temenoff, Y. Tabata, A.I. Caplan, A.G. Mikos, Injectable biodegradable hydrogel composites for rabbit marrow mesenchymal stem cell and growth factor delivery for cartilage tissue engineering, Biomaterials 28 (2007) 3217–3227.
[36] M.M.C. Bastings, S. Koudstaal, R.E. Kieltyka, Y. Nakano, A.C.H. Pape, D.A.M. Feyen, et al., A fast pH-switchable and self-healing supramolecular hydrogel carrier for guided, local catheter injection in the infarcted myocardium, Adv. Healthc. Mater. 3 (2014) 70–78.
[37] D.A. Ossipov, S. Piskounova, O.P. Varghese, J.N. Hilborn, Functionalization of hyaluronic acid with chemoselective groups via a disulfide-based protection strategy for in situ formation of mechanically stable hydrogels, Biomacromolecules 11 (2010) 2247–2254.
[38] P. Orth, D. Zurakowski, D. Wincheringer, H. Madry, Reliability, reproducibility, and validation of five major histological scoring systems for experimental articular cartilage repair in the rabbit model, Tissue Eng. C Methods 18 (2012) 329–339.